Available online at www.sciencedirect.com
SCIENCE DIRECT®
Journal of Chromatography A, 1063 (2005) 171–180
JOURNAL OF CHROMATOGRAPHY A
www.elsevier.com/locate/chroma

Cosorption effect in gas chromatography: flow fluctuations caused by adsorbing carrier gases☆

Daniel Matuszak, Glen D. Gaddy, Gregory L. Aranovich, Marc D. Donohue*

Department of Chemical and Biomolecular Engineering, The Johns Hopkins University, 3400 North Charles Street, Baltimore, MD 21218, USA

Received 6 July 2004; received in revised form 12 November 2004; accepted 19 November 2004
Available online 8 December 2004

Abstract

Adsorbing carrier gases have a number of advantages in analytical and preparative gas chromatography, such as clearer detector signals and higher column efficiencies. This work shows that adsorbing carrier gases also may be useful because they cause the mobile phase flow rate to become unsteady after injecting a small amount of sample. This work shows that a 100 μL sample of helium can liberate enough carbon dioxide carrier gas from a zeolite 5A packed column at 373 K, that the departure from the steady-state flow rate had an upper lobe area of 586 μL of carrier gas. This was confirmed by coupling a modified Langmuir kinetic model with the Ergun equation.

Keywords: Carrier gas; Sorption effect; Thermal conductivity detection; Flame ionization detection; Ultraviolet absorbance detection; Signal amplification; Peak asymmetry; Langmuir kinetic model; Ergun equation; Nonlinear chromatography; Adsorption dynamics

1. Introduction

Chromatographic separations rely on differences in multi-component adsorption dynamics. The science of multi-component adsorption has been studied since Langmuir and Brunauer, Emmett, and Teller [1]. However, as interest in more advanced separations and analyses increases, knowledge of multi-component adsorption in chromatography will become increasingly important. This work investigates the influence of multi-component gas adsorption dynamics on convective momentum transport in the mobile phase. In particular, this work examines how and when small perturbations in partial pressure can produce major variations in the effluent flow rate.

The assumption that the mobile phase flow rate remains constant after injection of sample is often appropriate in chromatography, especially if the sample is small and helium is the carrier gas. However, helium is not always selected for the mobile phase [2–11]. For example, humid nitrogen and carbon dioxide have been used as carrier gases to increase the retention of primary amines [8]; ammonia has been used as a carrier gas to increase the retention of organic acids of low molecular mass [9]; and binary mobile phases containing carbon dioxide have been used extensively in supercritical fluid chromatography (SFC) and high-performance liquid chromatography (HPLC) [12]. The choice of carrier gas is important because it dictates the column's efficiency [13,14], the sizes and shapes of detector signals [15–17], and the ease of downstream purification. This can be advantageous, but sometimes at the expense of this steady-flow assumption as shown in this paper.

Fluctuations in the mobile phase velocity and pressure have been studied previously. Bosanquet and Morgan examined changes in local flow velocity due to the sorption of sample [18] and are cited for terming this phenomenon the "sorption effect" [19,20]. Scott [21], Haarhoff and van der Linde [22] studied the local pressure changes in a column upon passage of sample. Peterson and Helfferich discussed changes

☆ This article is the result of work prepared under contract to the U.S. Government. By acceptance of this article, the publisher and/or recipient acknowledges the U.S. Government's right to retain a nonexclusive, royalty-free license in and to any copyright covering this paper.

* Corresponding author. Tel.: +1 410 516 6821; fax: +1 410 516 5510.
E-mail address: donohue@jhu.edu (M.D. Donohue).

0021-9673/$ – see front matter © 2004 Published by Elsevier B.V.
doi:10.1016/j.chroma.2004.11.064

in local, mobile phase velocity upon the arrival of a concentration band [23]. Buffham et al. measured such changes in flow rate and pressure [24]. Buffham and co-workers developed the method of sorption effect chromatography [25–27]. Yeroshenkova et al. [28], and Helfferich and Carr [29] noted how chromatograms can depend on the sorption effect. Jennings et al. [30], and Blumberg [31] explained the disparity of flow velocity in the column due to gas compression, whereas Shen and Lee [32] observed flow disparity caused by phase transitions. Many theories and methods that may deduce information about the stationary phase are based on the premise that there are differences in the linear velocity within the mobile phase. For example, the tracer-pulse technique [33] and sorption effect chromatography were developed to determine adsorption isotherms; they can be classified in the categories of perturbation gas chromatography and inverse gas chromatography [34–37]. The sorption effect continues to be used in gas–solid columns, but with the new focus of heterogeneous catalysis [38,39].

A common idea in these works is that a local stimulus (e.g., a change in the sample's concentration) can cause variations in the local flow velocity or pressure. This paper discusses a different kind of flow phenomenon: when an adsorbing carrier gas is used, a small amount of sample can affect the flow ahead of it, and perhaps behind it, by causing desorption of a larger amount of carrier gas—the sorption behavior of the carrier gas, rather than of the sample, affects the flow rate. This is complementary to the sorption effect and, for this reason, we call this phenomenon the cosorption effect. It can occur in the presence of a non-adsorbing sample such as helium, and may be useful in inverse gas chromatography or in applications where signal amplification is important.

Evidence for the cosorption effect arises in various applications, because it is an example of fundamental, multicomponent adsorption dynamics. In concentrated absorbers, significant increases in flow rates and entrainment occur while placing the system on standby operation [40]. This is the cosorption effect—placing absorbers on standby consists of replacing the feed stream with an inert stream, which can be considered an "injection" of a large sample. This effect can lead to mechanical damage and potentially dangerous and unacceptable exhausts to the environment [41]; and it causes premature and asymmetric breakthrough curves [42]. Furthermore, the pressure and flow transients can influence product formation in adsorptive reactors [43]. Here, the cosorption effect is discussed in the context of gas chromatography. Because it has not been explored in this context, it may be useful, and it can be very significant in analytical and preparative applications.

This paper demonstrates the cosorption effect in packed columns with carbon dioxide carrier and weakly-adsorbing samples; and it discusses how the effect is not limited to these systems. Consequently, the cosorption effect also is relevant to the science of SFC; which currently is exploring the effects of small amounts of helium in carbon dioxide carrier [44,45], and which has had a growing interest in developing packed-column SFC methods [46].

2. Fundamentals

The presence of sample can cause a flow fluctuation by influencing the sorption behavior of the carrier gas. After an injection of sample, fluctuations in the sample's and carrier's partial pressure occur as the sample passes each stage of the column. Consequently, the carrier desorbs and readsorbs at each stage with a net rate that is proportional to the slope of its isotherm. If the small amount of sample liberates large amounts of carrier while passing over the stationary phase, the cumulative amount of desorbed carrier can significantly alter the mobile phase flow rate. This effect is most significant in the presence of a non-adsorbing sample.

When both the sample and the carrier adsorb, the flow fluctuation depends on the difference between the rates of sample sorption and carrier sorption. The total pressure at each stage does not change if the sample is replaced immediately by an equivalent amount of carrier, and then vice versa. However, the total pressure increases at each stage if the rate of carrier desorption is greater than the rate of sample adsorption. As the sample passes the stages, the cumulative amount of desorbed carrier can be significant enough to change the effluent flow rate.

Fig. 1 demonstrates the cause of flow fluctuation in an activated-carbon column at 298 K when nitrogen sample is injected while using carbon dioxide carrier gas. In this illustration, it is assumed that the nitrogen and carbon dioxide adsorption isotherms are their pure fluid isotherms. If mass transfer is not rate-limiting, the decrease and increase of carbon dioxide's partial pressure will cause desorption and readsorption of carbon dioxide, respectively, as illustrated by the

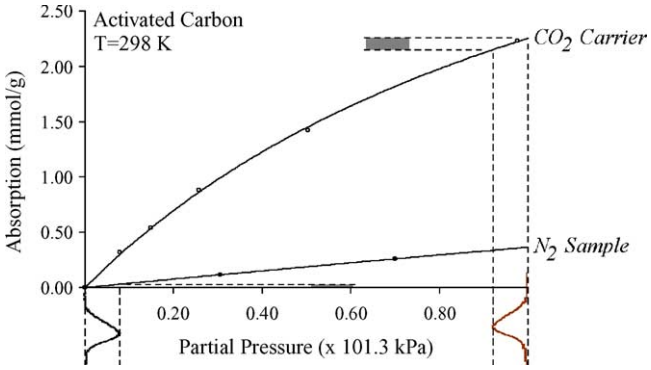

Fig. 1. Pure fluid adsorption isotherms of carbon dioxide and nitrogen on activated carbon [55]. An injection of nitrogen causes a perturbation in nitrogen's partial pressure, causing a complementary perturbation in carbon dioxide's partial pressure at the column's inlet—these perturbations are drawn below the horizontal axis. Consequently, the amounts of nitrogen and carbon dioxide adsorption change. The dashed lines indicate changes in the partial pressures and adsorption of both nitrogen and carbon dioxide. The relative sizes of the shaded sections emphasize that more carbon dioxide desorbs than nitrogen adsorbs, causing the flow fluctuation.

dashed lines in Fig. 1. Since the amount of carbon dioxide desorption is larger than the amount of nitrogen adsorption at each stage in the column, the local density increases. This puts pressure on the adjacent stages of the column, reducing the influx from the previous stage and increasing the efflux to the next stage. Overall, the column's effluent flow rate increases as the sample passes through the stages. The reverse happens when carbon dioxide readsorbs, returning the column to a steady state after the sample passes. Since a small amount of nitrogen can liberate larger amounts of carbon dioxide at each stage of the column, the cumulative amount of desorbed carbon dioxide can cause a significant flow fluctuation at the column's outlet.

Conversely, a significant flow fluctuation does not occur if the amount of carrier desorption at each stage is less than the amount of sample adsorption. In this case, the small amount of sample does not liberate significant, accumulating amounts of carrier as it passes through the packed bed; it causes local pressure fluctuations due to the sample's sorption behavior. There is no obvious effect until the sample reaches the last stage of the stationary phase. A small perturbation may be observed with a sensitive pressure-transducer [22], when the sample desorbs from the last stage of the stationary phase. Buffham et al. explained this, and it is known as the sorption effect—the sorption of sample does not change the local gas density enough to see significant changes in the effluent's flow rate because the sample size is usually very small [18,19,24].

When using adsorbing carrier gases, large changes in flow rate can occur without being observed. This can be the case when using thermal conductivity detection (TCD), ultraviolet (UV) absorbance detection, or flame ionization detection (FID). The sensitivity of TCD is proportional to the detector's filament current. Usually, the filament current is set large enough to detect the sample peak, small enough to minimize deterioration of the filament, but not large enough to sense changes in the effluent flow rate. However, if the filament current is large, the anomalous signals that result can be mistakenly attributed to the mixture's thermal conductivity because they can resemble hydrogen–helium signals [15,16]. Second, a UV detector does not sense changes in the fluid flow rate because the absorbance of light depends only on the fluid's composition. However, the sample's peak shape would be affected if the flow rate is transient while the sample is being detected downstream of the column—the transient behavior can continue after the sample leaves the column if the rate of carrier readsorption is slow. Last, in the case of FID, a small fraction of column effluent is diverted to the detector before being mixed with flame. Flow fluctuations are diminished by the restriction that splits off a sample of effluent from the main stream, and again by the mixing with flame that is supplied at a larger rate than the effluent sample. We do not know how common the cosorption effect is, but we hope that the reader would check for it with other detectors and flow meters.

In the following sections, the cosorption effect will be demonstrated experimentally and theoretically. Excellent agreement with experiments was attained using a modified Langmuir kinetic model [47] of nonlinear chromatography, in a modeling approach that uses the Ergun equation [48].

3. Experimental

3.1. Materials and apparatus

Pure argon, nitrogen, hydrogen, and helium were used as samples. Carbon dioxide was the carrier gas. A packed bed of zeolite 5A adsorbent (Supelco, 80–100 mesh) was formed in a 0.476 cm i.d. aluminum column of 12 cm total length. The packing was distributed by agitation with an etching pen; it was secured at both ends with a small amount of quartz wool.

A Varian 3700 gas chromatograph was used. Fig. 2 illustrates the experimental apparatus. The carrier gas was split to provide a reference stream for differential TCD. The other carrier gas stream was directed to the zeolite-packed column. Injections of sample were made at upstream column pressure using a sample valve with a sample volume of 100 μL. The sample loop was 0.159 cm i.d. and, therefore, the sample passed through an expanding coupling before entering the 0.476 cm i.d. column. Tubing between the column and the detector also was 0.476 cm i.d. aluminum.

The heating elements maintained the oven temperature at 373 K. The zeolite column's inlet and outlet pressures were 104.8 kPa and atmospheric pressure, respectively. The steady-state carbon dioxide flow rate was 23.07 ± 0.15 mL/min. The TCD detector's bridge current was 105 mA. The detector temperature was 403 K.

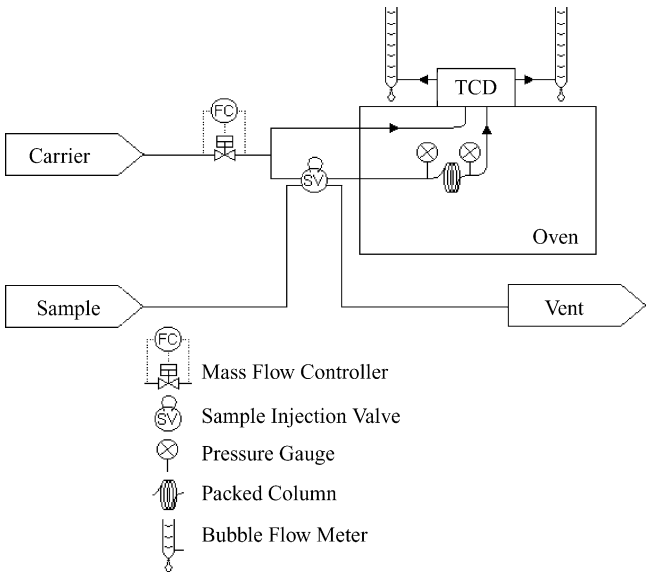

Fig. 2. Schematic of apparatus. The carrier gas is split to provide a reference stream for differential TCD. Sample is introduced to the column with a sample valve that has a 100 μL sample loop maintained at the column's inlet pressure. Bubble meters monitor the steady-state flow rates.

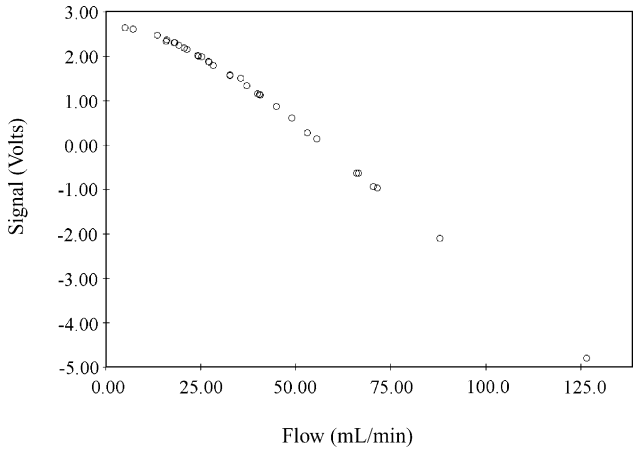

Fig. 3. Correlation of TCD signal to carbon dioxide flow rate.

3.2. Measurements and calibration

A soap bubble meter was used to measure the steady-state flow rate of the gas. TCD was used to sense changes in the flow rate and in the composition at the column's outlet. To study the behavior for each sample, three chromatograms were recorded using different lengths of extra-column tubing immediately downstream of the column. Additional post-column tubing serves in a qualitative mass balance—the injected mass of sample experiences additional residence time before the detector. Therefore, when varying the post-column tube length, a motile signal (a signal on the chromatogram that moves with the sample's post-column residence time) is the detector's response to the sample, and a stationary signal is the detector's response to the flow fluctuation.

The TCD signal was recorded as a function of the flow rate of carbon dioxide. These data appear in Fig. 3. Although each value of signal corresponds to a particular value of flow rate, the chromatograms may not begin at the signal corresponding to 23.07 mL/min because the detector was reset between trials. Resetting the detector changed the values of the signals in Fig. 3 but did not affect the shape of the curve.

3.3. Experimental results

Pure argon, nitrogen, hydrogen, and helium were injected while using carbon dioxide carrier gas and different post-column tube lengths. Figs. 4–7 show that two distinct signals occur for each sample. One signal appears stationary, while the time of the other signal depends on the length of additional post-column tubing. There was overlap between the two signals when no additional post-column tubing was used. This overlap resulted in a ∼33% increase of peak area for the helium and hydrogen samples.

Fig. 8 compares the chromatograms recorded after injections of various samples into the zeolite column with a post-column tube length of 164 cm. Carbon dioxide was the carrier gas. A steady baseline signal was obtained for the carbon dioxide sample. Injections of other samples produced two

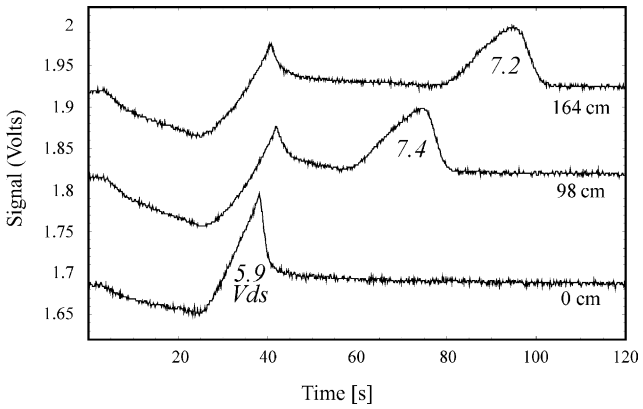

Fig. 4. Argon sample—chromatograms obtained by injecting argon into the zeolite column while using carbon dioxide carrier gas and two different lengths of post-column tubing. Peak areas are shown in units of volt-deciseconds.

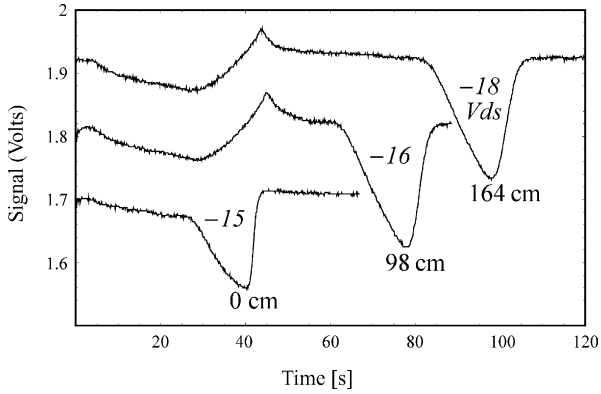

Fig. 5. Nitrogen sample.

signals in each chromatogram: one caused by the flow fluctuation, and one caused by the sample band. The signals caused by flow fluctuations are similar for all samples; each signal decreases, increases above the baseline, then returns toward the baseline because the flow rate increases, decreases below the steady-state value, then returns to the steady-state flow rate. On the other hand, the signals caused by the sample bands depend on the sample's shape and thermal conduc-

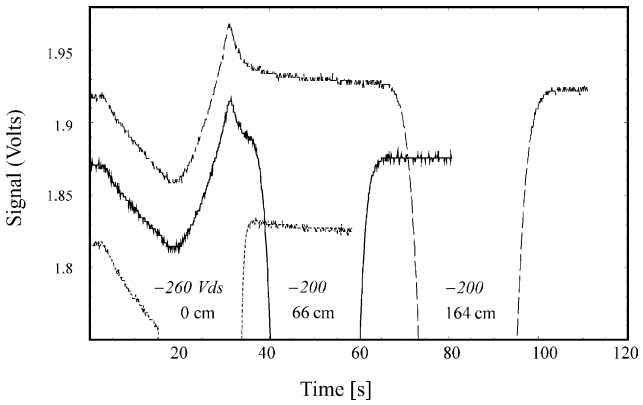

Fig. 6. Hydrogen sample.

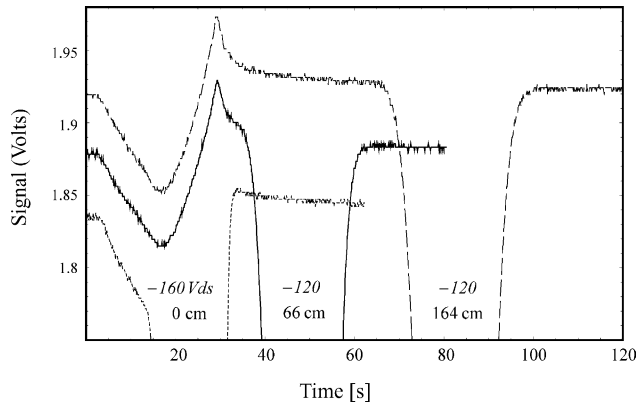

Fig. 7. Helium sample.

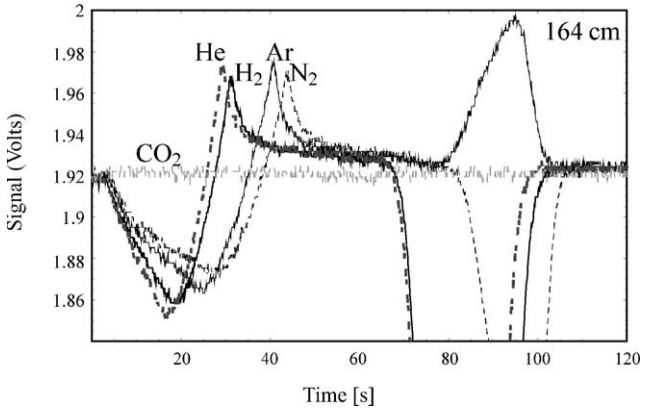

Fig. 8. Chromatograms obtained after injections of various samples into the zeolite column while using carbon dioxide carrier gas and a post-column tubing of 164 cm. Chromatogram after injection of carbon dioxide remains at the baseline signal.

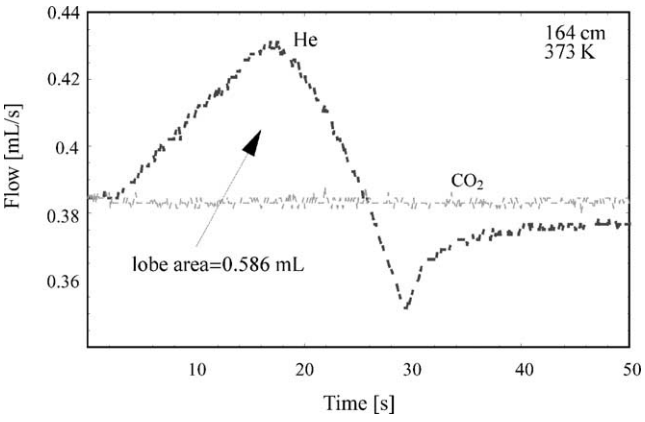

Fig. 9. Effluent flow rates after injections of helium and carbon dioxide samples into the zeolite column while using carbon dioxide carrier gas and a post-column tubing of 164 cm. The flow rate remains constant after injecting the carbon dioxide sample. For the helium sample, the flow rate deviates from the steady-state value. The deviation is characterized by an upper lobe area of 586 μL of carrier gas.

tivity. Helium, hydrogen, and nitrogen have higher thermal conductivities than the carrier gas; their signals appear below the baseline signal. Argon has a lower thermal conductivity than the carrier; its signal appears above the baseline signal.

The data in Fig. 3 were used to analyze the signal associated with the flow fluctuation caused by the helium sample; the signal after injecting carbon dioxide sample was analyzed for reference; carbon dioxide was the carrier gas. The flow rates are shown in Fig. 9. After injecting carbon dioxide, the flow rate remained at the steady-state value. After injecting helium, the flow rate increased as much as 12.8% above the steady-state value, and decreased as much as 7.9% below the steady-state value. For a 100 μL sample, the departure from the steady-state flow rate had an upper lobe area of 586 μL of carrier gas.

4. Kinetic model of packed-bed dynamics

This section describes a modified Langmuir kinetic model (LKM) of nonlinear chromatography for the packed-bed column shown in Fig. 10. The assumptions are that (1) the mobile phase is a binary ideal-gas mixture; (2) adsorption kinetics are Langmuirian; (3) only the carrier gas adsorbs onto the stationary phase; (4) the viscosity is constant; (5) the system is isothermal; (6) there are no radial gradients in the column as this is a one-dimensional problem; (7) the bed's particle diameter and porosity are spatially invariant; and (8) convection prevails over diffusion in the axial dimension. This model does not assume local equilibrium.

4.1. Modified Langmuir kinetic model

The cosorption effect is modeled with a modified LKM of nonlinear chromatography [47]. The LKM is a classical model that describes dynamics within a chromatography column by using material balances for each species in each phase:

$$\left[\frac{\partial(yP)}{\partial t}\right]_z = -\left[\frac{\partial(yPu)}{\partial z}\right]_t - \frac{\rho_a RT}{\varepsilon}\left(\frac{\partial q}{\partial t}\right)_z \quad (1)$$

$$\left[\frac{\partial((1-y)P)}{\partial t}\right]_z = -\left[\frac{\partial((1-y)Pu)}{\partial z}\right]_t \quad (2)$$

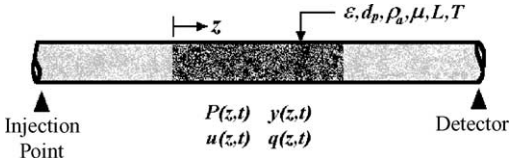

Fig. 10. Sketch of the modeled packed column with relevant variables and parameters.

$$\left(\frac{\partial q}{\partial t}\right)_z = \frac{1-\varepsilon}{\tau N_o \sigma^2 \rho_a d_p}\left[\left(\frac{yP}{\rho^c RT}\right)\left(1-\frac{q}{q^{sat}}\right) - \left(\frac{q}{q^{sat}}\right)\left(1-\frac{yP}{\rho^c RT}\right)e^{-U/RT}\right] \quad (3)$$

In Eqs. (1)–(3), t is the time; z is the position as measured from the beginning of the bed; y is the mole fraction of carrier; P is the pressure; u is the superficial velocity of the mobile phase; q is the amount of adsorbed carrier; ρ_a is the adsorbent's bed density; RT is the thermal energy; ε is the bed porosity; d_p is the adsorbent's particle diameter; τ is the period of molecular vibration of the adsorbate while on the stationary phase; N_o is Avogadro's number; σ is the adsorbate's Lennard–Jones diameter; ρ^c is the critical density of the adsorbate; q^{sat} is the adsorption capacity; and U is the adsorbate's energy of interaction with the adsorbent's surface. Eq. (3) is a nonequilibrium rate equation that was obtained by adapting a lattice density function approach for diffusion [49]. The regular assumption that the flow rate is constant would preclude using a momentum balance, allowing determination of all variables with Eqs. (1)–(3) only. Up to this point, the modeling approach is classical.

In this problem, the variables P, u, y, and q must be determined; they depend on both z and t. As a result, four independent equations are required. The Ergun equation [48] is the fourth equation:

$$\left(\frac{\partial P}{\partial z}\right)_t = -\frac{(1-\varepsilon)}{\varepsilon^3 d_p}\left[\frac{150\mu(1-\varepsilon)}{d_p}u + 1.75\frac{P}{RT}u^2\right] \quad (4)$$

where μ is the viscosity of the mobile phase. The Ergun equation considers friction factors in packed beds, accounting very well for momentum transport in both laminar and turbulent regimes [48].

4.2. Boundary and initial conditions

The boundary conditions were set at the inlet ($z = 0$) and outlet ($z = L$) of the packed bed:

$$P(0,t) = P_o \quad (5)$$

$$P(L,t) = P_L \quad (6)$$

$$y(0,t) = 1 - ae^{-b(t-t_o)^2} \quad (7)$$

In Eq. (7), the parameters a and b were adjusted to deliver 100 μL of sample at a time t_o. Initially, the column operates at steady state with pure carrier gas, which causes a pressure gradient and adsorbs to the stationary phase:

$$y(z,0) = 1 \quad (8)$$

$$P(z,0) = \sqrt{P_o^2 + (P_L^2 - P_o^2)\left(\frac{z}{L}\right)} \quad (9)$$

$$q(z,0) = \frac{q^{sat}}{1-[1-(\rho^c RT/P(z,0))]e^{-U/RT}} \quad (10)$$

Table 1
Modified Langmuir kinetic model's parameters

	Value	Units	Comments
d_p	0.000145	m	Specified, MS5A (Supelco, 80–100 mesh)
ε	0.425555	–	Calculated from measurement
L	0.12	m	Measured
ρ_a	721	kg/m^3	Measured
T	373	K	Measured
P_o	102845	Pa	Estimated from measurement
P_L	102338	Pa	Estimated from measurement
ρ^c	465	kg/m^3	Published [50], CO_2 critical density
q^{sat}	572.25	mol/kg	Fitted from CO_2 data [53] at low pressure
U	6400	J/mol	Fitted from CO_2 data [53] at low pressure
w_m	0.044	kg/mol	Published, molecular weight of CO_2
σ	4×10^{-10}	m	Published [48], LJ diameter of CO_2
τ	10^{-13}	s	Published [51], period of surface vibration
μ	0.001733	Pa s	Published [50], viscosity of CO_2
t_o	65	s	Adjustable parameter
a	0.015	–	Adjustable parameter
b	0.0146	1/s	Adjustable parameter

Eqs. (9) and (10) are the steady-state solutions of Eqs. (3) and (4), respectively. The pressure gradient is not constant because the fluid is compressible. Second, the carrier adsorption profile depends on the pressure profile, $P(z, t)$.

4.3. Parameters

The parameters were chosen to model an injection of helium into a packed bed with carbon dioxide carrier, as described in Section 3. Table 1 lists and describes the parameter values chosen for Eqs. (1)–(7). The values of d_p, ρ_a, L, and T were measured during experiment or specified by the supplier. The values of the following parameters were obtained from the literature: ρ^c [50], w_m [50], σ [48], τ [51] and μ [50]. Eq. (4) was used to determine the value of ε from flow measurements in the Section 3. This combination of parameters yields values for ε and for the ratio $150\mu(1-\varepsilon)^2/\varepsilon^3 d_p^2$ that agree very well with reported values for sand-packed pressure-swing adsorbers [52]. Adsorption data [53] were used to obtain reasonable values of q^{sat} and U for the range of pressure modeled here. The values of P_o and P_L were estimated from experiment—the experimentally-measured inlet and outlet pressures differed at the bed due to additional frictional losses from the fittings and the quartz wool that were used to support the bed. The values of a, b, and t_o were chosen to perturb the carrier's partial pressure with 100 μL of sample, at a constant total pressure and at an arbitrary time t_o.

4.4. Model's results

Fig. 11 shows the adsorption isotherm used in the model. The left peak in Fig. 12 shows the perturbation in the carrier's mole fraction at the column's inlet; this peak's width is ∼16 s at half-height; although the perturbation is symmetric and centered at 65 s, the carrier mole fraction begins to differ visibly from the steady-state value at approximately 45 s. The

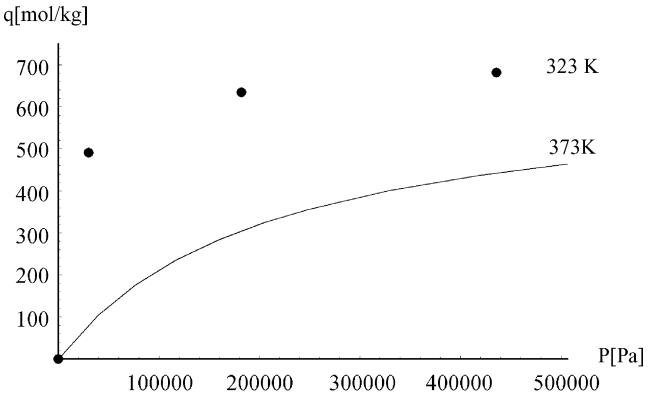

Fig. 11. Experimental (323 K) and modeled (373 K) adsorption isotherms.

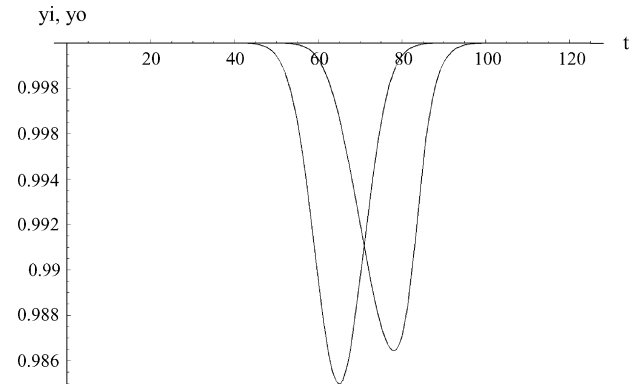

Fig. 12. Concentration bands at the column inlet (i) and outlet (o). The mole fraction of carrier gas (y) is spiked with a symmetric sample of 100 μL of inert gas that is centered at 65 s. The outlet concentration is for the model that assumes 2% contactable surface area.

resultant flow fluctuation appears in Fig. 13—the experimental data was shifted to account for an additional hold-up time of 50 s caused by the perturbation centered at the arbitrary time t_o. The model predicts a much larger fluctuation but it qualitatively resembles the experimental data—the flow rate increases, passes through a maximum, decreases below the steady-state value, then returns toward the steady-state value. This discrepancy can be explained by the fact that most of

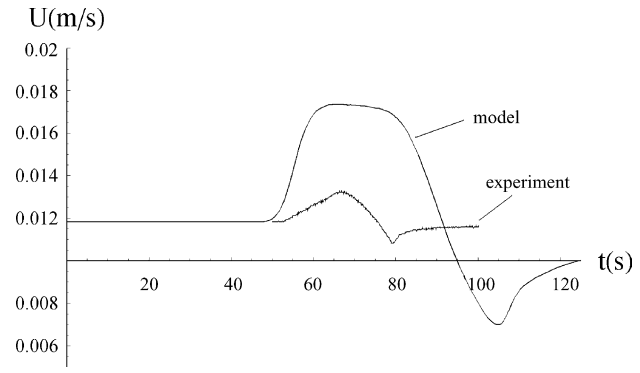

Fig. 13. Comparison of the experimental and modeled flow fluctuations. The model over-predicts the fluctuation because it assumes that all the adsorbent's surface area is exposed to the passing sample.

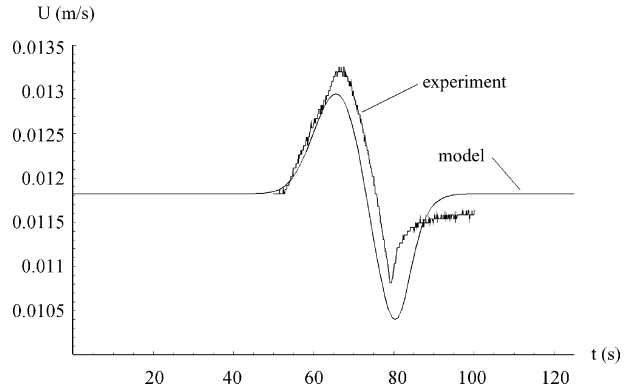

Fig. 14. Comparison of the experimental and modeled flow fluctuations. The model assumes that only 2% of the area available for equilibrium adsorption is contacted by the passing sample.

the adsorbent's area, which is available for equilibrium adsorption, lies beneath the outermost surface of the adsorbent particles—only a fraction of this area is exposed to the passing sample. This is normal for porous adsorbents such as the zeolite 5A used in Section 3. Assuming that only 2% of the adsorbent is contacted by the injected sample, the calculation was repeated with a different adsorption isotherm for the "exposed" adsorbent. This adsorption isotherm differs from the original isotherm in the adsorption capacity, such that $q^{sat}_{exposed} = 0.02q^{sat}$. Fig. 14 shows the resultant fluctuation, which agrees very well with the measured fluctuation. Furthermore, the modeled fluctuation has an upper lobe area of 524 μL of carrier gas, which compares well with the experimentally measured value of 586 μL. This lobe area is greater than 500% of the sample size. Fig. 14 shows that the model's flow fluctuation lasts approximately 40 s, and Fig. 12 indicates a maximum in the outlet concentration at approximately 28 s after the fluctuation begins—therefore, the inert sample exists the column during the flow fluctuation.

5. Discussion

The cosorption effect is a significant fluctuation in the mobile phase flow rate that occurs after sample is injected into a column while using an adsorbing carrier. Therefore, it is important to the analysis of chromatograms, which can have additional peak asymmetry and amplification due to flow fluctuations. Evidence for the cosorption effect has been observed in concentrated absorbers, which experience significant increases in flow rates and entrainment while being placed on standby operation [40–42]. In the gas chromatography setting described earlier, the cosorption effect was reproduced, measured, and modeled. The flow fluctuations were observed with TCD, which was calibrated for flow measurement as shown in Fig. 3. The signal is inversely proportional to the effluent flow rate.

Often in chromatography, TCD is used to sense changes in gas composition. In Section 3, TCD was used to sense

changes in both the gas flow rate and the gas composition. To avoid interference between the two types of signals, extra post-column tubing was used to delay the arrival of sample at the detector, and to demonstrate the consequences of interference. Figs. 4–7 show two detector responses for the cases using post-column tubing. Since the sample's residence time changes when using different lengths of post-column tubing, it follows that the motile signals are caused by the sample's concentration band. The stationary signals are caused by flow rate changes due to the sorption of carbon dioxide; they are not caused by a response from the mass flow controller or from the same phenomenon that produces anomalous hydrogen–helium TCD signals [15,16]. This is supported by the observance of steady baseline signals after injecting a carbon dioxide sample while using carbon dioxide carrier gas, as shown in Fig. 8—a flow fluctuation was not sensed because this sample did not affect the sorption of carrier gas, and a concentration band was not detected because this sample is indistinguishable from the carrier. The steady baseline signals obtained after injecting carbon dioxide also indicate that a pressure peak was not present after injection.

The reason for the lack of a pressure peak also explains why the effluent flow rate does not change necessarily when the sample first arrives at the adsorbent. A pressure peak is the detector's response to a small pressure fluctuation caused by using the sample valve. It occurs immediately after injecting a sample because a pressure wave travels at the speed of sound between the sample valve and detector. However, the packed bed suppresses the pressure wave by reflecting and absorbing the wave. Therefore, the pressure peak can be reduced to an amplitude that is less than the variability in baseline signal, making it unobservable. For the same reason, pressure changes caused by desorption and readsorption of carrier gas at the column's inlet may not be sensed to an appreciable amount at the column's outlet. If the pressure at the column's outlet does not change appreciably when sample arrives at the inlet, then a flow fluctuation cannot be sensed at the detector. After the sample advances in the column, the changes of pressure due to carrier gas sorption can be sensed at the column's outlet and at the detector. This is evident from Figs. 12 and 14, in which the sample arrives at the bed at approximately 45 s, and the flow fluctuation begins at approximately 53 s.

One reviewer noted that "the retention time for an unsorbed solute such as helium should be [. . .] less than 3 s. Yet the retention time shown for helium in Fig. 7 is over 20 s with no delay tubing." The model in Fig. 12 also shows that the retention time of an unsorbed solute (the hold-up time) is 13.1 s. The difference between 20 and 13.1 s is partially caused by the unavoidable dead volume between the column and the detector. Nevertheless, both experiments and theory show that the cosorption effect significantly increases the hold-up time beyond 3 s. We regret not having an explanation for this counter-intuitive observance.

Note from Figs. 6 and 7 that when the concentration band arrives at TCD detector during a flow fluctuation, the area of the overall peak can be more than 30% larger than the area of the undisturbed, concentration band's peak. This happens because both flow rate and composition change simultaneously at the TCD filament, cooling the filament differently than it would if only the composition had changed. This can introduce systematic error when studying peak shapes, peak areas, or residence time distributions. The problem can be avoided by offsetting the desired signals from the flow transient's signal. As long as axial diffusion of the concentration band is not significant, inserting empty tubing downstream of the stationary phase will reduce this systematic error.

Signals caused by the cosorption effect may be masked by other signals when using TCD. Furthermore, these fluctuations are not apparent when the TCD bridge current is too low or when using other detection methods, such as FID or UV detection. Low TCD bridge currents make the detector less sensitive. For FID, flow fluctuations that propagate from the column's outlet are insignificant compared to the flow of the flame. In the case of a UV detector, flow fluctuations are not sensed.

During the cosorption effect, the flow rate increases because the rate of carrier desorption is larger than the rate of sample adsorption; it decreases because the rate of carrier readsorption is larger than the rate of sample desorption. This explains the quicker flow response for a helium sample than for a nitrogen sample, as shown in Fig. 8—nitrogen has a greater rate of sorption than helium, which does not adsorb appreciably at 373 K. Since the TCD signal is inversely proportional to the effluent flow rate, the signal decreases, increases, then returns to baseline in Fig. 8, because the flow rate increases, decreases, then returns to the steady-state flow rate, as shown for a helium sample in Fig. 9.

Figs. 8 and 9 reveal the usefulness of the cosorption effect. The areas of the upper lobes in Fig. 9 show that amplification of more than 500% of the sample size is possible. This was demonstrated with zeolite 5A, which has much area concealed from the quickly passing sample. Using an adsorbent with larger pores while operating slightly into the capillary condensation regime would make this effect more dramatic. Furthermore, the size and shape of the flow fluctuation contains information about the sample and the stationary phase; with a thermal conductivity detector, Nelsen and Eggertsen showed that measuring the flow changes caused by sorption in gas chromatography can determine the specific surface area better than the traditional BET approach [54]. Fig. 8 shows the signal's dependence on the type of sample.

In the modified Langmuir kinetic model, the cosorption effect was modeled for a column that closely resembled the column used in Section 3. However, this effect occurs in all columns that empirically obey Eqs. (1)–(4), including capillary columns—although the Ergun equation is for packed beds, the Ergun equation has the same phenomenological form for the friction factor f as the Hagen–Poiseuille law in the laminar flow regime, namely $f = k/Re$, where k is a constant and Re is the Reynolds number [48]. In the LKM, the heat of adsorption was determined from the equilibrium ad-

sorption isotherm, which was modeled after carbon dioxide at 373 K as shown in Fig. 11. A symmetric concentration spike of sample was introduced to the column, as shown in Figs. 12 and 13 shows that the model over-predicts the flow fluctuation; this model's fluctuation had an upper lobe area greater than 9000% the sample size. This amplification would be very useful but it does not occur with zeolite 5A, because the sample does not contact all the surface area available for equilibrium adsorption. Assuming that the sample only contacts 2% of this area yields much better agreement with experiment, as shown in Fig. 14. This contact area may be increased by slowing the mobile phase velocity or by using a different adsorbent.

6. Conclusion

Chromatographic experiments using a thermal conductivity detector and carbon dioxide for the carrier gas show that significant variations of gas flow rate can occur after injection in a packed column. Very good agreement was obtained with a modified Langmuir kinetic model of nonlinear chromatography. The flow fluctuations are attributed to desorption and readsorption of the carrier gas upon passage of sample. A small sample can liberate a much larger amount of adsorbed carrier, causing a measurable response in the effluent flow rate. For the case of a helium sample and carbon dioxide carrier gas, the positive departure from the steady-state flow rate has time-integrated area that is greater than 500% of the sample volume.

Acknowledgements

G.L.A. and M.D.D. would like to acknowledge support from the U.S. Department of Energy under grant DE-FG02-87ER13777. D.M. would like to acknowledge the Howard Hughes Medical Institute for a summer research fellowship, and Building Service 32BJ Thomas Shortman Training, Scholarship and Safety Fund, for a graduate fellowship. D.M. thanks Dr. Maeve McCarthy, from Murray State University, for a very helpful and encouraging discussion of P.D.E. solving techniques. Also we would like to thank the anonymous reviewer who noticed that the cosorption effect causes major differences between observed and expected hold-up times.

References

[1] J.H. de Boer, The Dynamical Character of Adsorption, Clarendon Press, Oxford, 1968.
[2] A. Nonaka, Anal. Chem. 44 (1972) 271.
[3] J.F. Parcher, J. Chromatogr. Sci. 21 (1983) 346.
[4] M. Abdel-Rehim, L. Zhang, M. Hassan, H. Ehrsson, J. Microcol. Sep. 5 (1993) 537.
[5] L. Ghaoui, K. Pell, K. Chritz, R.N. Loomis, J. High Resolut. Chromatogr. 18 (1995) 157.
[6] E. Alpay, N. Haq, L.S. Kershenbaum, N.F. Kirkby, Gas Sep. Purif. 10 (1996) 25.
[7] M. Abdel-Rehim, J. Microcol. Sep. 11 (1999) 63.
[8] V.G. Berezkin, T.P. Popova, Russ. Chem. B 48 (1999) 1118.
[9] V.G. Berezkin, V.R. Alishoev, A.A. Korolev, I.V. Malyukova, J. Chromatogr. A 903 (2000) 173.
[10] Y.G. Slizhov, M.A. Gavrilenko, T.N. Matveeva, Petrol. Chem. 41 (2001) 131.
[11] S. Impens, K. De Wasch, H. De Brabander, Rapid Commun. Mass Spectrom. 15 (2001) 2409.
[12] P.S. Wells, S. Zhou, J.F. Parcher, Anal. Chem. 75 (2003) 18A.
[13] T. Tsuda, N. Tokoro, D. Ishii, J. Chromatogr. 46 (1970) 241.
[14] T. Tsuda, D. Ishii, J. Chromatogr. 87 (1973) 554.
[15] P.G. Jeffery, P.J. Kipping, Gas Analysis by Gas Chromatography, Pergamon Press, New York, 1972.
[16] C.J. Cowper, A.J. DeRose, The Analysis of Gases by Chromatography, Pergamon Press, Oxford, New York, 1983.
[17] A. Karmen, R.L. Bowman, I. Mccaffrey, Nature 193 (1962) 575.
[18] C.H. Bosanquet, G.O. Morgan, Vapour-Phase Chromatography, Butterworths, London, 1957.
[19] B.A. Buffham, G. Mason, G.D. Yadav, J. Chem. Soc., Faraday Trans. 1 81 (1985) 161.
[20] J. Roles, G. Guiochon, J. Phys. Chem. 95 (1991) 4098.
[21] R.P.W. Scott, Anal. Chem. 36 (1964) 1455.
[22] P.C. Haarhoff, H.J. van der Linde, Anal. Chem. 37 (1965) 1742.
[23] D.L. Peterson, F.G. Helfferich, J. Phys. Chem. 69 (1965) 1283.
[24] B.A. Buffham, G. Mason, R.I. Meacham, J. Chromatogr. Sci. 24 (1986) 265.
[25] G. Mason, B.A. Buffham, Proc. R. Soc. London A: Mater. Phys. Eng. Sci. 452 (1996) 1263.
[26] G. Mason, B.A. Buffham, M.J. Heslop, Proc. R. Soc. London A: Mater. Phys. Eng. Sci. 453 (1997) 1569.
[27] G. Mason, B.A. Buffham, Proc. R. Soc. London A: Mater. Phys. Eng. Sci. 452 (1996) 1287.
[28] G.V. Yeroshenkova, S.A. Volkov, K.I. Sakodynskii, J. Chromatogr. 198 (1980) 377.
[29] F.G. Helfferich, P.W. Carr, J. Chromatogr. 629 (1993) 97.
[30] W. Jennings, E. Mittlefehldt, P.P. Stremple, Analytical Gas Chromatography, Academic Press, San Diego, CA, 1997.
[31] L.M. Blumberg, Chromatographia 43 (1996) 73.
[32] Y.F. Shen, M.L. Lee, Anal. Chem. 70 (1998) 737.
[33] S.H. Hyun, R.P. Danner, Ind. Eng. Chem. Fund. 24 (1985) 95.
[34] C.J. Glover, W.R. Lau, AIChE J. 29 (1983) 73.
[35] H.C. Song, J.F. Parcher, Anal. Chem. 62 (1990) 2313.
[36] N.A. Katsanos, E. Arvanitopoulou, F. Roubani-Kalantzopoulou, A. Kalantzopoulos, J. Phys. Chem. B 103 (1999) 1152.
[37] T.I. Bakaeva, C.G. Pantano, C.E. Loope, V.A. Bakaev, J. Phys. Chem. B 104 (2000) 8518.
[38] B.A. Buffham, K. Hellgardt, M.J. Heslop, G. Mason, Chem. Eng. Sci. 55 (2000) 1621.
[39] B.A. Buffham, K. Hellgardt, M.J. Heslop, G. Mason, D.J. Richardson, Chem. Eng. Sci. 57 (2002) 953.
[40] P. Gunaseelan, P.C. Wankat, Ind. Eng. Chem. Res. 40 (2001) 850.
[41] P. Gunaseelan, P.C. Wankat, Ind. Eng. Chem. Res. 41 (2002) 5775.
[42] B.K. Arumugam, J.F. Banks, P.C. Wankat, Adsorption 5 (1999) 261.
[43] B.K. Arumugam, P.C. Wankat, Adsorption 4 (1998) 345.
[44] J.F. Parcher, Y. Xiong, J. Chromatogr. A 986 (2003) 129.
[45] M. Roth, J. Chromatogr. A 1037 (2004) 369.
[46] Y. Wu, J. Liq. Chromatogr. Rel. Technol. 27 (2004) 1203.
[47] G. Guiochon, S.G. Shirazi, A.M. Katti, Fundamentals of Preparative and Nonlinear Chromatography, Academic Press, Boston, 1994.
[48] R.B. Bird, W.E. Stewart, E.N. Lightfoot, Transport Phenomena, Wiley, New York, 1960.

[49] D. Matuszak, G.L. Aranovich, M.D. Donohue, J. Chem. Phys. 121 (2004) 426.
[50] R.H. Perry, D.W. Green, J.O. Maloney, Perry's Chemical Engineers' Handbook, McGraw-Hill, New York, 1997.
[51] D.A. Porter, K.E. Easterling, Phase Transformations in Metals and Alloys, Chapman & Hall, London, New York, 1992.
[52] B.D. Crittenden, J. Guan, W.N. Ng, W.J. Thomas, Chem. Eng. Sci. 49 (1994) 2657.
[53] Y. Wakasugi, S. Ozawa, Y. Ogino, J. Colloid Interf. Sci. 79 (1981) 399.
[54] F.M. Nelsen, F.T. Eggertsen, Anal. Chem. 30 (1958) 1387.
[55] F. Dreisbach, R. Staudt, J.U. Keller, Adsorption 5 (1999) 215.